STRUCT: A Second-Generation URANS Approach for Effective Design of Advanced Systems

Citation: Baglietto, Emilio, et al. "STRUCT: A Second-Generation URANS Approach for Effective Design of Advanced Systems." Proceedings of the ASME 2017 Fluids Engineering Division Summer Meeting, July 30-August 3, 2017, Waikoloa, Hawaii, ASME, 2017, p. V01BT12A004. © 2017 ASME

As Published: http://dx.doi.org/10.1115/FEDSM2017-69241

Publisher: ASME International

Persistent URL: http://hdl.handle.net/1721.1/117004

Version: Final published version: final published article, as it appeared in a journal, conference proceedings, or other formally published context

Proceedings of the ASME 2017 Fluids Engineering Division Summer Meeting
FEDSM2017
July 30-August 3, 2017, Waikoloa, Hawaii, USA

FEDSM2017-69241

STRUCT : A SECOND-GENERATION URANS APPROACH FOR EFFECTIVE DESIGN OF ADVANCED SYSTEMS

Emilio Baglietto
Department of Nuclear Science and Engineering
Massachusetts Institute of Technology
Cambridge, MA 02139, USA

Giancarlo Lenci
Dominion Engineering, Inc.
Reston, VA, USA

Davide Concu
Advanced Design Technology, Ltd
London, UK

ABSTRACT

This work presents the recently developed STRUCT hybrid turbulence model and assesses its potential to address the poor grid consistency and limited engineering applicability typical of hybrid models. Renouncing the ability to consistently bridge RANS, LES and DNS based on the computational grid size, we aim at addressing the engineering design needs with a different mindset. We opt to leverage the robustness and computational efficiency of URANS in all nearly homogeneous flow regions while extending it to locally resolve complex flow structures, where the concept of Reynolds averaging is poorly applicable. The proposed approach is best characterized as a second generation URANS closure, which triggers controlled resolution of turbulence inside selected flow regions. The resolution is controlled by a single-point parameter representing the turbulent timescale separation, which quantitatively identifies topological flow structures of interest. The STRUCT approach demonstrates LES-like capabilities on much coarser grids, and consistently increases the accuracy of the predictions from the baseline URANS at increasing grid finesse. The encouraging results show the potential to support effective design application through resolution of complex flow structures while controlling the computational cost. The ultimate objective is to continue improving the robustness and computational efficiency while further assessing the accuracy and range of applicability.

INTRODUCTION

A clear trend is observable in the industrial application of Computational Fluid Dynamics (CFD), moving away from classic RANS-based steady-state simulations and into scale-resolving models capable of capturing complex unsteady flow features that bear important information on the performance of the analyzed systems. The challenge for the industry has been to identify and adopt methods capable of providing increased flow resolution while limiting the computational cost in order to remain amenable to effective design exploration.

Hybrid LES/RANS remains the predominant approach in the turbulence community [1][2][3], where the variety and complexity of the proposals is astounding, but their industrial applicability still limited. Overall, hybrid models have demonstrated increased accuracy on specific test cases, and in combination with purposely crafted computational grids. However, in practical applications, when non-perfect meshes are adopted, or mixed flow configurations are encountered, existing hybrid models have shown to often produce unacceptably large errors, significantly higher than those of URANS closures [4][5][6]. Most importantly, the models have evidenced a fundamental lack of grid convergence on all complex flow cases, often amplified by the adoption of grid related hybridization parameters. Due to these severe limitations, hybrid models are still impracticable for high-cost/risk engineering applications.

While a systematic review of all hybrid proposals is out of the scope of this paper, valuable reviews are available in [7][8][9]. Here we classify the approaches into large families in order to discuss their fundamental ideas and assumptions motivating the proposed new approach. Two essential hybrid models, among the first ones to be developed, are the very-large-eddy simulation (VLES) proposed by Speziale [10] and the detached-eddy simulation (DES) proposed by Spalart and co-workers [11]. Practically all hybrid models can be reduced in terms of one, or a combination of both these methods. While VLES aims at providing a global model that can behave as a DNS, LES or URANS based on the computational grid size, all DES incarnations zonally transition between URANS and LES solutions. The limitations of both concepts in industrial applications are immediately apparent.

On the one side, a global approach requires selecting a priori the desired level of resolution and constructing ad-hoc

computational grids. While the a priori selection is applicable to specific flow regions, it may not be practicable across the complete computational domain of large-scale industrial applications. The models usually produce considerably different levels of scale resolution and accuracy at varying grid size, with a limited range of acceptable solutions and non-monotonic convergence. The most successful example of this family of models is the partially averaged Navier-Stokes (PANS) by Girimaji and co-workers [12].

On the other hand, DES approaches have been very successful in applications where massively separated flow regions exist, and well-defined length scale separation between flow regions allows models to clearly define their 'zonal' blending. More recent incarnations of the approach [15][16] have in part reduced the sensitivity to the computational mesh, but need remains for the user to recognize a priori the separation regions and adopt LES-like local grid refinement. When applied to wall-bounded flows and complex systems, the scale separation requirements are not easily met and LES regions cannot are not easily identified a priori. In blind industrial benchmarks this limitation has resulted in evident failure of the method [6], including the more recent scale-adaptive simulation (SAS)[13][14].

Departing from the classic approach of a model capable of bridging RANS and LES based on the computational grid size, the STRUCT method is grounded on the choice of leveraging the robustness and computational efficiency of URANS in all nearly homogeneous flow regions, while extending the concept to locally resolve complex flow structures. The proposed approach [25] triggers controlled resolution of turbulence inside selected flow regions, leveraging a single-point parameter representing the turbulent timescale separation, which quantitatively identifies topological flow structures of interest.

The soundness of the approach is demonstrated first through its application to classic hybrid-turbulence challenge flow cases. The assessment focuses first on the fundamental applicability of the flow structure identification and its robustness at varying computational grid resolutions. Further, the work addresses the challenge of a general formulation, proposing and evaluating dynamic implementations applicable to general unstructured finite volume solvers. Efficiency, robustness and overall performance of the approach are evaluated qualitatively and quantitatively.

STRUCTURE-BASED RESOLUTION

The proposition brought forward in this work addresses the industrial robustness need of hybrid formulations by leveraging the URANS framework and extending it to overcome its fundamental limitations evidenced by Pope in 1975 [18]:

- the inadequacy of the isotropic-viscosity hypothesis, which can be addressed by introducing a nonlinear eddy viscosity formulation (NLEVM)
- the inapplicability of the effective-viscosity approach to rapidly varying flows.

The latter point, which limits the applicability of URANS to quasi-homogeneous flows, is simply discussed by considering the ensemble averaging operation, which assumes statistically stationary fluctuations. In flows for which this condition is met, scale separation exists between turbulence and slowly varying phenomena, such as a gently varying inlet velocity. Basic URANS models are not meant to be used when residual fluctuations are far from being statistically stationary. This happens, for example, in flows with large-scale anisotropic vortical structures, curvature, intermittency, buoyancy, swirl, which are very frequent in engineering applications.

The STRUCT approach [19] addresses this challenge in a distinctive way: by using a NLEVM in flow regions where its underlying assumptions are met while eliminating the URANS inconsistency by locally resolving a significant portion of the turbulent fluctuations in regions with lack of scale separation. The local resolution is achieved without introducing any dependency on the computational mesh scale, either explicit (e.g. DES) or implicit (e.g. LES). Such proposition well fits the definition of Second Generation URANS Models (2G-URANS), introduced by Fröhlich and Von Terzi [8].

Local Resolution

The rationale for local resolution is a central aspect of the current proposal. In STRUCT, the resolved flow regions are determined by comparing two time scales: one defined for resolved deformation and one for modeled scales.

Resolved time scale

The resolved time scale is defined based on the second invariant of the resolved velocity gradient tensor, which is:

$$\bar{I}\bar{I} = -\frac{1}{2}\frac{\partial \bar{u}_i}{\partial x_j}\frac{\partial \bar{u}_j}{\partial x_i} = \frac{1}{2}(\bar{\Omega}_{mn}\bar{\Omega}_{mn} - \bar{S}_{mn}\bar{S}_{mn}) \qquad (1)$$

where the resolved shear and rotation rates are:

$$\bar{S}_{ij} = \frac{1}{2}\left(\frac{\partial \bar{u}_i}{\partial x_j} + \frac{\partial \bar{u}_j}{\partial x_i}\right), \bar{\Omega}_{ij} = \frac{1}{2}\left(\frac{\partial \bar{u}_i}{\partial x_j} - \frac{\partial \bar{u}_j}{\partial x_i}\right) \qquad (2)$$

The resolved time scale is expressed in the form of a frequency to allow numerical values of $\bar{I}\bar{I}$ equal to zero:

$$f_r = \sqrt{|\bar{I}\bar{I}|} \qquad (3)$$

The approach based on the second invariant of the resolved velocity gradient tensor has several useful advantages for hybrid turbulence modeling [25]:

A. It is one of the simplest nonzero invariants applicable to incompressible flows describing flow deformation through velocity gradients. Galilean and frame rotation invariance properties are necessary for a suitable turbulence model.
B. It has low values in simple shear flows, i.e. those flows in which the velocity vector, orthogonal to the wall, only varies in the wall-normal direction. This behavior ensures URANS modeling near the wall in simple flows, which is a common feature of DES and other hybrid models.
C. Its instantaneous counterpart is widely used in the flow topology literature to describe coherent structures.
D. Its value can be used to detect regions of rapid distortion caused either by strain or rotation.

Modeled scale

The working variable for the modeled flow can be expressed as a frequency f_m or as a time scale $t_\mathrm{m} = 1/f_\mathrm{m}$. Its definition is:

$$\frac{1}{f_\mathrm{m}} = t_\mathrm{m} \equiv \langle t_{\mathrm{m},0} \rangle \tag{4}$$

where the chevrons represent a generic averaging operation, applied to a parameter providing information on the modeled turbulent scales. In k-ε models (which are leveraged in this work) let us define $t_{\mathrm{m},0}$ based on modeled turbulence fields:

$$t_{\mathrm{m},0} = \frac{k_\mathrm{m}}{\varepsilon} \tag{5}$$

The averaging operation in Eq. 4 varies depending on the STRUCT implementation considered and serves the purpose of removing the smallest local variations of $t_{\mathrm{m},0}$ caused by resolved eddies, thus delivering a smooth t_m field around those eddies.

Hybridization

The hybridization in the model can then be controlled as the amount of modeled versus resolved scales. This approach can be expressed by the simple general formulation:

$$r = \begin{cases} 1 & , \quad h \leq 1 \\ \phi & , \quad h > 1 \end{cases} \tag{6}$$

The parameter r is the ratio between the TKE modeled by the hybrid turbulence closure and the TKE modeled by URANS. The function ϕ is a resolution parameter and h is an activation parameter triggering hybrid turbulence. In the most generic formulation, the two parameters ϕ and h are arbitrary functions of space and time. The definition used here for h is the following:

$$h \equiv \frac{f_\mathrm{r}}{f_\mathrm{m}} = t_\mathrm{m} f_\mathrm{r} \tag{7}$$

The choice of parameter ϕ is dependent on the specific implementation of the model.

Finally, the hybridization is implemented following a straightforward approach adapted from the hybrid proposal by Perot and Gadebusch [16], which directly reduces the overall eddy viscosity through the reduction parameter, allowing the model to be extremely portable and easy to adapt to different baseline URANS closures:

$$\nu_\mathrm{t} = C_\mu \frac{k_\mathrm{m}^2}{\varepsilon} r \tag{8}$$

In order to illustrate the STRUCT strategy in comparison to other turbulence approaches, the concept is applied in Fig. 1 to the image of a tree [25]. The size of branches corresponds to the size of eddies. Resolved scales are in full color while residual scales are faded.

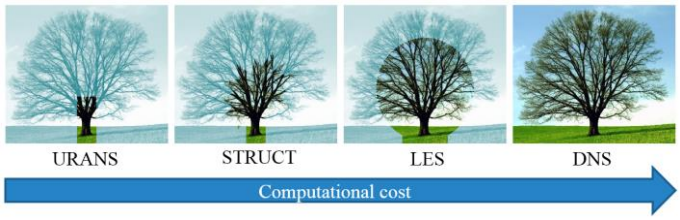

Figure 1. Illustration of the STRUCT approach's rationale.

BASELINE URANS MODEL

In order to address the first URANS limitation outlined by Pope [18], a NLEVM formulation is adopted which develops from his original proposal. This selection allows avoiding the large overestimation of turbulent viscosity in complex strains, typical of eddy viscosity models, which would hamper the full effectiveness of the hybrid formulation. The cubic NLEVM closure proposed by Baglietto and Ninokata [20][21] is selected and is based on the original proposal by Shih, Zhu and Lumley [22], while reformulating the model coefficients on the base of their physical interpretation, leveraging DNS data to extend the generality of the formulation. The residual stress anisotropy tensor expands the linear formulation by adding quadratic and cubic terms.

$$a_{ij} = \tau_{ij} - \frac{2}{3} k_\mathrm{m} \delta_{ij} = \nu_t \left(-2\bar{S}_{ij} + q_{ij} + c_{ij} \right) \tag{9}$$

$$q_{ij} = 4C_1 \frac{k_\mathrm{m}}{\varepsilon} \left[\bar{S}_{ik}\bar{S}_{kj} - \frac{1}{3}\delta_{ij}\bar{S}_{kl}\bar{S}_{kl} \right] + 4C_2 \frac{k_\mathrm{m}}{\varepsilon} \left[\bar{\Omega}_{ik}\bar{S}_{kj} + \bar{\Omega}_{jk}\bar{S}_{ki} \right] + 4C_3 \frac{k_\mathrm{m}}{\varepsilon} \left[\bar{\Omega}_{ik}\bar{\Omega}_{jk} - \frac{1}{3}\delta_{ij}\bar{\Omega}_{kl}\bar{\Omega}_{kl} \right] \tag{10}$$

$$c_{ij} = 8C_4 \frac{k_\mathrm{m}^2}{\varepsilon^2} \left[\bar{S}_{ki}\bar{\Omega}_{lj} + \bar{S}_{kj}\bar{\Omega}_{li} \right] \bar{S}_{kl} + 8C_5 \frac{k_\mathrm{m}^2}{\varepsilon^2} \left[\bar{S}_{kl}\bar{S}_{kl} - \bar{\Omega}_{kl}\bar{\Omega}_{kl} \right] \bar{S}_{ij} \tag{11}$$

The non-constant coefficients used in (10) and (11) are:

$$C_\mu = \frac{C_{a0}}{C_{a1} + C_{a2}\bar{S}^* + C_{a3}\bar{\Omega}^*} \tag{12}$$

$$C_1 = \frac{C_{NL1}}{(C_{NL6} + C_{NL7}\bar{S}^{*3})C_\mu} \tag{13}$$

$$C_2 = \frac{C_{NL2}}{(C_{NL6} + C_{NL7}\bar{S}^{*3})C_\mu} \tag{14}$$

$$C_3 = \frac{C_{NL3}}{(C_{NL6} + C_{NL7}\bar{S}^{*3})C_\mu} \tag{15}$$

$$C_4 = C_{NL4} C_\mu^2 \tag{16}$$

$$C_5 = C_{NL5} C_\mu^2 \tag{17}$$

where:

$$\bar{S}^* = \frac{k}{\varepsilon}\sqrt{2\bar{S}_{ij}\bar{S}_{ij}} \quad , \quad \bar{\Omega}^* = \frac{k}{\varepsilon}\sqrt{2\bar{\Omega}_{ij}\bar{\Omega}_{ij}} \tag{18}$$

and the model constants from [20], are shown in Table I.

Table I. Cubic NLEVM constants

C_{a0}	C_{a1}	C_{a2}	C_{a3}	C_{NL1}	C_{NL2}	C_{NL3}	C_{NL4}	C_{NL5}	C_{NL6}	C_{NL7}
0.667	3.9	1.0	0.0	0.8	11.0	4.5	-5.0	-4.5	1000.0	1.0

DEMONSTRATING THE STRUCT CONCEPT

The hybridization of the STRUCT model requires defining an averaging operation for the modeled time scale (eq. 4) and a resolution parameter ϕ. At first, the model applicability can be

demonstrated by calculating the averaged modeled time scale from a precursory URANS analysis and varying the resolution parameter to evaluate the effects of increased resolution. These tests allow evidencing the robustness of the strategy on varying grid resolutions and topology. While only partial results are presented here, all details are available in [25].

Flow past a square cylinder

The flow past a square cylinder test case by Lyn et al. [23] represents a common benchmark for all hybrid models. The square cylinder side size is 4 cm, and the Reynolds number is 21,400. A structured 10.5 mm mesh was used, refined by 50% in a region around and past the obstacle in combination with a low-Re treatment [24]. The total size of this mesh is 646,000 cells, on which URANS grid convergence has been achieved.

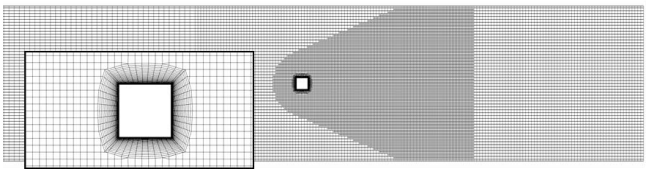

Figure 2. Flow past a square cylinder, computational grid.

The precursor URANS simulation allows estimating the controlled STRUCT parameters. Geometric averaging of $t_{m,0}$ in the region around the square cylinder leads to the value used here of $t_m = 0.33$ s. The resolution parameter for this case is reduced to an extremely low value $\phi = 1 \times 10^{-10}$ to evaluate the model performance with no residual stresses in the activation region.

The analysis of the time-averaged velocity profiles in the x-direction (Fig. 3), confirms the effect of the hybridization in the wake region near the obstacle, where STRUCT produces results in close agreement with the experiment. It is useful to also observe how the cubic URANS recovers the correct solution as the flow moves away from the 'high-deformation' region near the obstacle. This evidence is of further support to the proposed local hybridization. The linear URANS model predicts a wake characterized by negative time-averaged velocity-x, as a consequence of an excessive eddy viscosity.

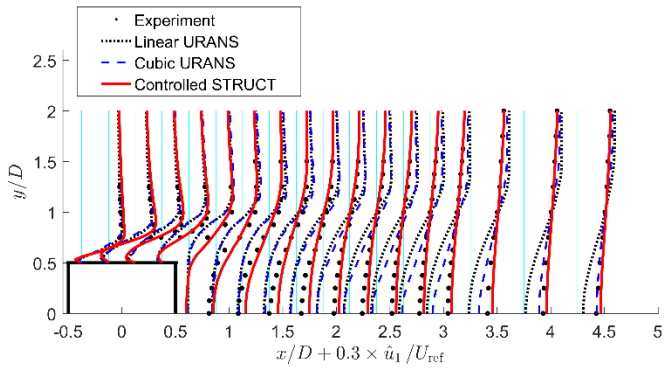

Figure 3. Flow past a square cylinder, time-averaged velocity. $\hat{u}_1$ profiles

The variance of velocity with respect to time average is shown in Fig. 4 and quantifies the effect of the hybridization. The STRUCT results are in close agreement with the experiment, as the largest contribution to the variance originates from the resolved component of velocity variance, which is not captured by the URANS predictions.

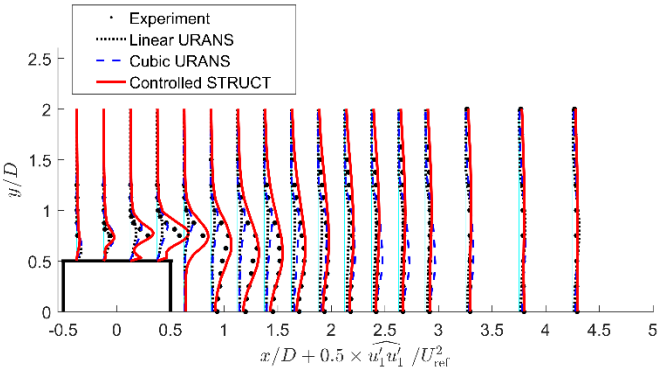

Figure 4. Flow past a square cylinder, time variance of velocity, $\widehat{u_1'u_1'}$ profiles.

In order to demonstrate the generality of the approach, the model activation regions are shown in Fig. 5 for strongly varying grid finesse. In particular the grids adopt polyhedral control volumes to further demonstrate insensitivity to cell topology.

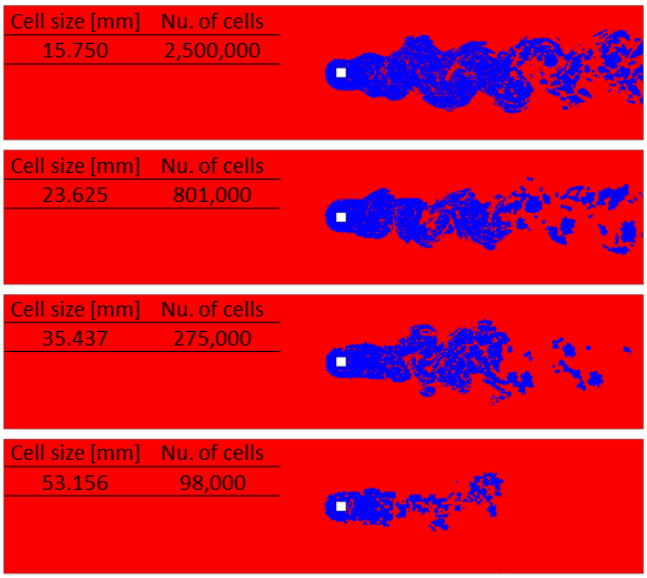

Figure 5. STRUCT activation regions for four polyhedral grids, ordered from the finest to the coarsest.

The URANS regions are shown in red, while the hybrid turbulence activation regions are shown in blue. In such a clear-cut case, it is evident how the model can select the activation regions without the need to depend on length scales or grid sizes. As expected, as the grid size increases (towards the bottom of the picture) the model will be less capable of resolving the unsteady 3-dimensional flow structures and the solution will revert back to the original URANS baseline. The demonstrated behavior of the STRUCT model is a key feature for its industrial application,

for which a "fail-safe" model is a strong requirement when the quality of the computational grid cannot be generally guaranteed. From a quantitative point of view, Fig. 6 confirms the discussed trends. The 3 finest grids (including the 10.5 mm trimmed grid from Fig. 2) produce very similar results, while the two coarsest polyhedral meshes asymptote back to the URANS results. The grid resolution in these cases is simply too coarse to allow resolution of relevant important scales, and the best that a model can do is to approach URANS-like predictions.

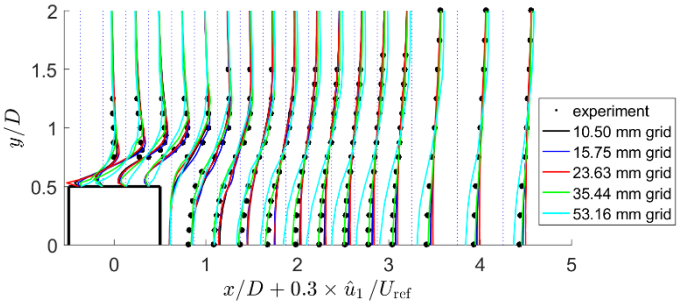

Figure 6. Controlled STRUCT grid sensitivity, time-averaged velocity $\hat{u}_1$ profiles.

Turbulent mixing in a T-junction

The T-junction mixing test case was selected for the first OECD/NEA-sponsored blind CFD benchmark [6] due to its relevance for industrial applications. The test case explores thermal striping causing fatigue in structural materials. This case is particularly useful as the blind benchmark clearly indicated the failure of both the DES and SAS methods. In all cases while LES provided excellent predictions, all applied hybrid approaches produced results far worse than their baseline URANS [6].

In the T-junction configuration, colder (19 °C) water flowing through a 140-mm-diameter pipe encounters an intersection where warmer (36 °C) water is injected through a smaller (100 mm) diameter pipe. The volumetric flow rate is 9×10^{-3} m^3/s for the cold stream and 6×10^{-3} m^3/s for the hot one. The URANS-converged computational mesh adopted is shown in Fig. 7 and contains 746,000 trimmed cells.

From the averaging of a precursor URANS simulation a value of $t_\mathrm{m} = 0.1$ s was obtained, while a larger value for $\phi = 0.6$ was applied. The URANS and STRUCT results are compared to the experiment, and further to an LES simulation with a base size of 1.5 mm (60 million cells), necessary to resolve 80% of the turbulent kinetic energy.

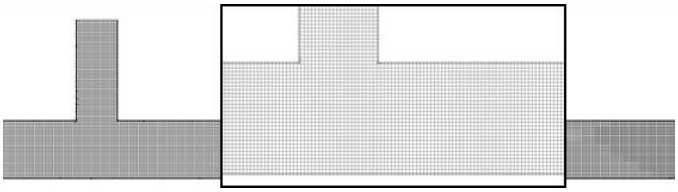

Figure 7. Turbulent mixing in a T-junction, computational grid.

An example of the results obtained is shown in Figure 8. Velocity profiles predicted by the STRUCT approach match the experiment closely adopting the same URANS coarse mesh, achieving similar accuracy compared to the fine-mesh LES, at a computational cost two orders of magnitude lower.

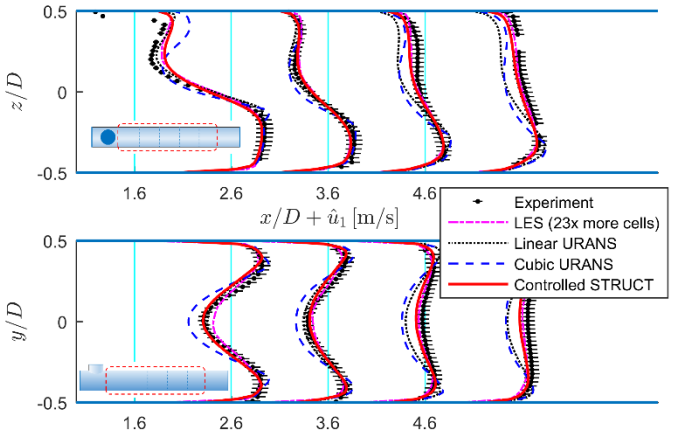

Figure 8. T-junction mixing, time-averaged velocity $\hat{u}_1$ profiles

SELF-ADAPTIVE IMPLEMENTATIONS

In order to fully generalize the applicability of the approach, both the averaging and the selection of the resolution parameters need to be performed adaptively in real time. For this particularly challenging task, in order to maintain optimal scalability on highly parallel computations we constrain the methods to only adopt single-point parameters.

STRUCT-Transport

In this formulation, the averaging operation is approximated through a convective-diffusive transport equation. The complete model is referred to as STRUCT-Transport (STRUCT-T). Extending the original proposal of Meneveau, Lund and Cabot [26], we adopt a differential operator to approximate a Lagrangian averaging. While Menevau and colleagues have limited their scope to a time averaging, here we extend to a differential operator in space and time. While the algebraic details are available in Lenci [25], the proposed averaging operation used to evaluate t_m is as follows:

$$\frac{\mathrm{d}t_\mathrm{m}}{\mathrm{d}t} + \boldsymbol{u} \cdot \boldsymbol{\nabla} t_\mathrm{m} = \frac{L^2}{T} \boldsymbol{\nabla}^2 t_\mathrm{m} + s \qquad (19)$$

where s is the source term to the averaging, and bounding is introduced to allow for greater model stability and adaptation to initial conditions.

$$s = \min\left(\max\left(\frac{1}{T}\left(t_{\mathrm{m},0} - t_\mathrm{m}\right), -\frac{2t_\mathrm{m}}{\Delta_t}\right), \frac{2t_\mathrm{m}}{\Delta_t}\right) \qquad (20)$$

The source term is clipped to ensure a value within its physical range. The length and time scales used for the averaging are defined based on local flow conditions as:

$$L = \sqrt{C}\frac{k_\mathrm{m}^{3/2}}{\varepsilon} \qquad (21)$$

$$T = \beta\frac{k_\mathrm{m}}{\varepsilon} \qquad (22)$$

The value $C = 0.09$ derives from the standard k-ε model.

The value for β used is 0.01 which demonstrated stable performance. This choice allows biasing the time-space averaging operation towards the space component. Boundary conditions are assigned so that at the inlet and walls $t_{\mathrm{m}} = t_{\mathrm{m},0}$. The same is also done for the initialization of t_{m}.

Dynamic strategy for the control coefficient

The control parameter ϕ defines the resolved-to-total TKE ratio in regions of STRUCT activation. In Eq. 7 the activation parameter h was calculated as a product between the two working variables f_{r} and t_{m}, while the control parameter ϕ was prescribed as constant. In a fully adaptive manner instead, both h and ϕ are now based on the product between the variables, and Eq. 6 is replaced by:

$$r = \min\left(\frac{1}{\alpha t_{\mathrm{m}} f_{\mathrm{r}}}, 1\right) \tag{23}$$

This idea corresponds to reducing the TKE ratio in the activation regions, based on a metric identifying scale overlap. The stronger the scale overlap, the lower is r. The calibration coefficient α is optimized to the value of 1.35.

The performance of the self-adaptive implementation is demonstrated here on the same test cases presented previously.

Flow past a square cylinder

The model activation and resolution obtained from the STRUCT-T approach is shown in Fig. 9 for the flow past a square cylinder test case. The ratio of modeled to total TKE reduces to nearly zero in the rapidly varying regions, consistent with the controlled model application.

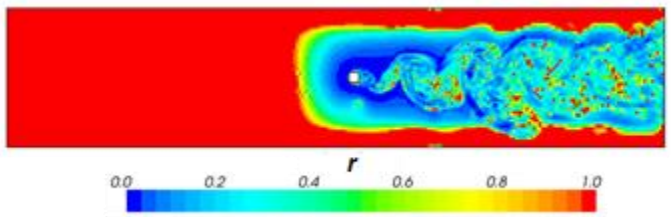

Figure 9. STRUCT-T activation, instantaneous scalar field, flow past a square cylinder.

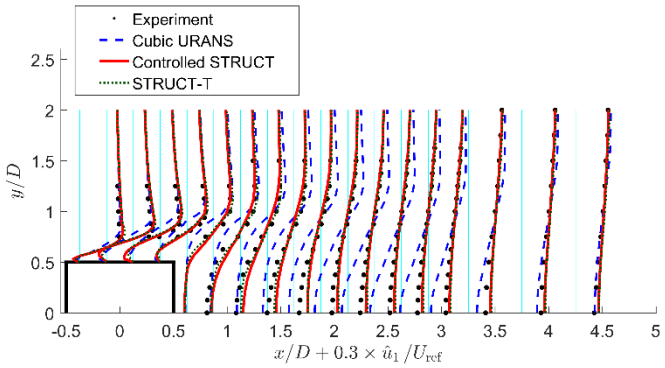

Figure 10. Flow past a square cylinder, STRUCT-T, time-averaged velocity $\hat{u}_1$.

Velocity profiles in Fig. 10 and 11 demonstrate the consistent performance of the STRUCT-T approach, with predictions very similar to the controlled STRUCT demonstration.

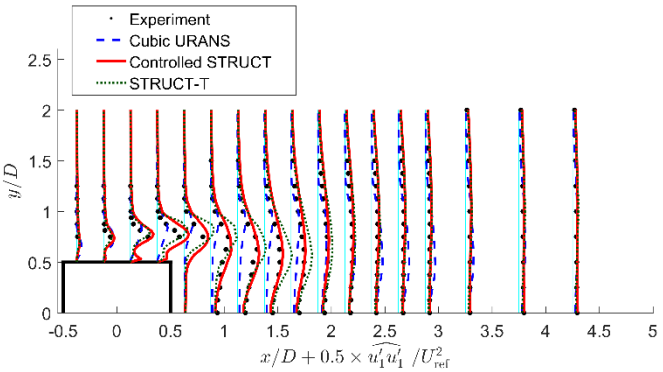

Figure 11. Flow past a square cylinder, STRUCT-T, time variance of velocity, $\widehat{u_1' u_1'}$ profiles.

Turbulent mixing in a T-junction

STRUCT-T results for the T-junction case, for the main time-averaged components of velocity, are shown in Fig. 12. An overall close agreement of STRUCT-T results with experimental data is shown, with a small deviation for the current implementation in comparison to the LES and experimental data.

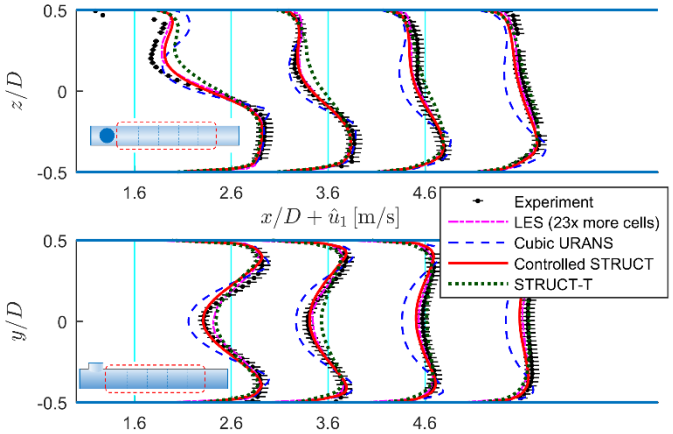

Figure 12. T-junction mixing, STRUCT-T, time-averaged velocity $\hat{u}_1$.

The first two data sections downstream the junction overestimate the velocity predicted at the center of the pipe. The performance is overall satisfactory as the model produced results similar to LES at a cost almost two orders of magnitude lower.

EXTERNAL AERODYNAMICS APPLICATIONS

While the STRUCT approach was originally developed for application to wall-bounded flows, the method is general and should carry its applicability to external flow cases. The main challenge expected is related to the averaging operation, which is now challenged by the dominant influence of the inlet boundary conditions. The model is therefore demonstrated for this case making use of a local averaging approach (the complete

discussion is available in [25]). Two model formulations are compared:

- STRUCT-L: where transported average is replaced by an averaging operation based on a truncated Taylor series expansion (the complete discussion is available in [25]). The resolution parameter ϕ is fixed at a value of 0.6, while f_m is dynamically estimated by means of the local average.
- STRUCT-Tau22: where the controlled averaging is coupled to a dynamic expression to define the resolution parameter. Its formulation is given in Equation 24 below and is clipped between a small positive number (10^{-10}) and 1:

$$\phi = \frac{1}{2(t_{\mathrm{m},0} f_{\mathrm{r}})^2 + 10^{-10}} \qquad (24)$$

In order to assess the STRUCT model potential, the well-known Ahmed body test case is adopted [27][28][29], and the challenging 25° slant angle configuration results are shown. The flow behavior is that of a 'bluff body', with two counter-rotating cone-shaped vortices separating downstream the slant.

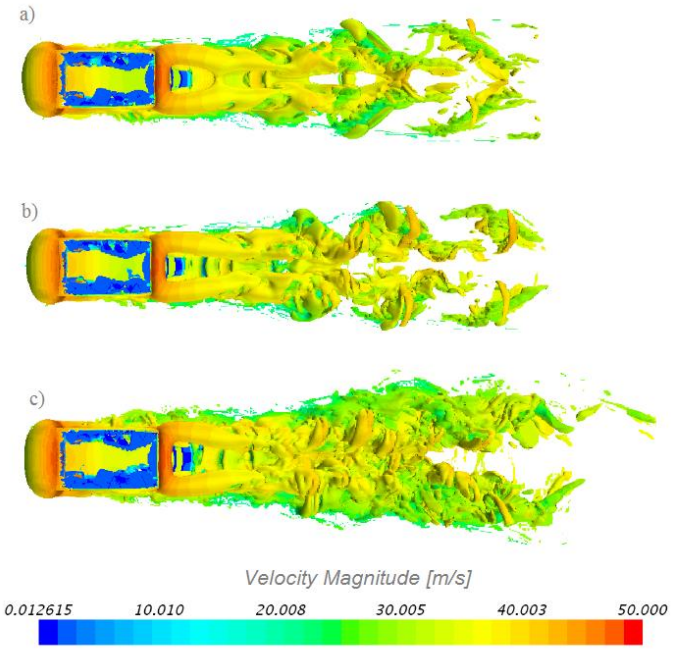

Figure 13: Q-Criterion iso-surfaces colored by the velocity magnitude, a) Cubic URANS b) STRUCT-L c) STRUCT-Tau22.

Figure 13 compares the wake predictions of the Cubic URANS models against the STRUCT approaches. While the cubic URANS does, to a minimal extent, resolve the wake region (as a considerable advancement from linear eddy viscosity models) only the STRUCT-Tau22 captures the wake appropriately. The flow in the wake is characterized by a uniquely compound behavior of the vortices, which are first directed downward and towards each other, and later move away from the mid-plane. The URANS-like results produced by the STRUCT-L model are explained by the selection for the parameter ϕ in the model as 0.6, which being conservatively high hinders complete resolution.

In order to compare the predictions of the different approaches in finer detail, the time-averaged velocity predictions against the measurements are shown in Figure 14.

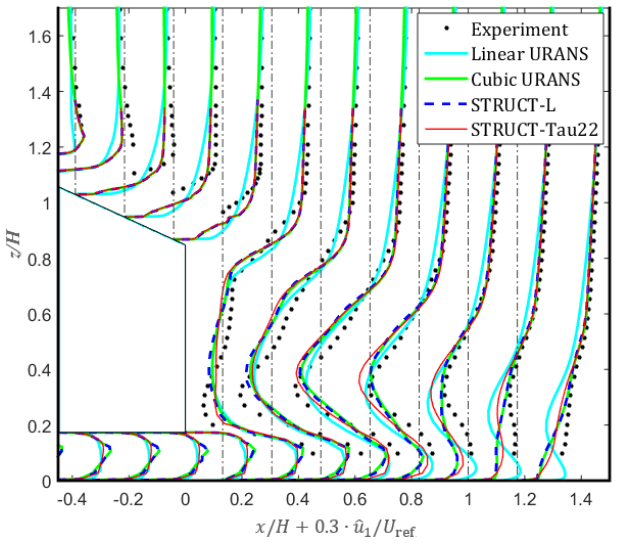

Figure 14: Ahmed Body (25° slant case), Plane y=0, time-averaged velocity, $\hat{u}_1$.

The time-averaged velocity results produced by the two STRUCT models are very close to those from cubic URANS. Results from those three models are in closer agreement with the experimental trends as compared to the linear URANS.

Finally, comparing the prediction of the overall drag coefficient C_D is important to appreciate the effect of the wake description and is done in Table 1.

Table 1: Drag coefficients

	C_D
Experiment	0.285
Cubic URANS	0.318
STRUCT-L	0.331
STRUCT-Tau22	0.302

The STRUCT-L results show the highest value of drag coefficient and generate the highest deviation of 16% with respect to the experimental value of $C_{D,exp} = 0.285$. This over-prediction is consistent the distribution of C_p on the back part and the slant (Fig. 15), where the contour peaks are significantly lower compared to the other two models. The Cubic URANS results display a lower deviation of 11.6% being still far from the acceptable range. The closest agreement in terms of drag coefficient prediction comes from the STRUCT-Tau22 model, showing the lowest deviation of 6% from the experiment, in accordance with the distribution of the highest range of C_p on the back part of the vehicle, shown in Figure 15.

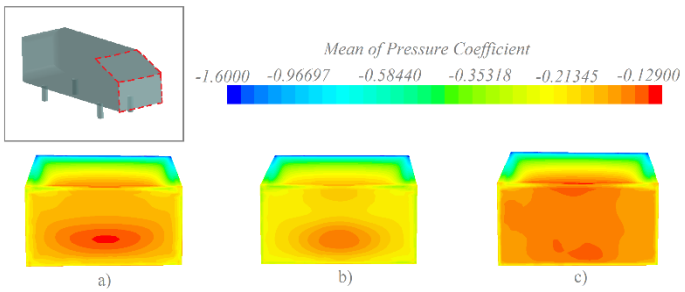

Figure 15: Distribution of the time-averaged C_p on the slant and rear surface a) Cubic URANS b) STRUCT-L c) STRUCT-Tau22.

CONCLUSIONS

A second-generation URANS closure was proposed for application to industrial flows. The new approach aims at delivering a considerable advancement in the robustness and applicability of hybrid turbulence models by relying on the efficiency of an extensively validated anisotropic k-e method, while locally introducing the necessary resolution of complex unsteady flow structures. Departing from existing ideas the proposed model does not leverage any grid dependent parameter, but triggers controlled resolution of turbulence only in regions of poor URANS applicability, while reverting to a URANS-like solution when rapidly varying structures are not identified.

The soundness of the approach has been demonstrated through its application to a variety of flow cases, including configurations that had until present not been addressed successfully by existing hybrid approaches. The assessment has focused on the fundamental applicability of the flow structure identification and its robustness at varying computational grid resolutions. In this work, results for the cases of flow past a squared cylinder and turbulent mixing in a T-junction have been briefly discussed. Further, the work has addressed the challenge of a general formulation, proposing and evaluating dynamic implementations applicable to general unstructured finite volume solvers. The potential of extending the applicability of the model to external aerodynamics simulation has also been discussed by presenting results for the well-known Ahmed body test case.

The work has demonstrated the LES-like capabilities of the STRUCT approach on much coarser grids, which allows a reduction on the total computing time between 50-100 folds. Most importantly, the presented cases have confirmed the expected consistent improvement in the results accuracy at increasing mesh resolution, which is fundamental to support effective industrial design applications. The results evidence the promising potential of the approach and motivate a continuing effort to further advance the accuracy and range of applicability while retaining the demonstrated robustness and computational efficiency.

ACKNOWLEDGMENTS

The authors gratefully acknowledge the financial support received from TerraPower, the U.S. Department of Energy, Skoltech, Areva, and the Theos J. Thompson Memorial Fellowship.

REFERENCES

[1] R. Manceau and J.P. Bonnet, (2003). Proc. 10th ERCOFTAC/IAHR/QNET-CFD Workshop on Refined Turbulence Modelling. Laboratoire d'études Aerodynamiques, UMR CNRS 6609, Université de Poitiers, France.

[2] H. Steiner, S. Jakirlic, G. Kadavelil, R. Manceau, S. Saric and G. Brenn, (2008). 13th ERCOFTAC Workshop on Refined Turbulence Modelling. Graz University of Technology, Austria.

[3] R. Manceau and S. Benhamadouche, (2011). 15th ERCOFTAC SIG15 Workshop on Turbulence Modelling. EDF at Chatou, France.

[4] L. Davidson, (2006). Evaluation of the SST-SAS model: Channel flow, asymmetric diffuser and axi-symmetric hill, in *Proceedings of the European Conference on Computational Fluid Dynamics (ECCOMAS CFD 2006)*, pp. 1–20.

[5] M. S. Gritskevich, A. V. Garbaruk, T. Frank, and F. R. Menter, (2014). Investigation of the thermal mixing in a T-junction flow with different SRS approaches, *Nuclear Engineering and Design*, vol. 279, pp. 83–90.

[6] B. L. Smith, J. H. Mahaffy, K. Angele, and J. Westin, (2011). Report of the OECD/NEA-Vattenfall T-Junction Benchmark exercise, NEA/CSNI/R(2011)5.

[7] P. Sagaut, (2006). Large Eddy Simulation for Incompressible Flows: An Introduction (Springer-Verlag Berlin and Heidelberg GmbH & Co.

[8] J. Fröhlich and D. Von Terzi, (2008). Hybrid LES/RANS Methods for the Simulation of Turbulent Flows, *Prog. Aerosp. Sci.* **44**, 349.

[9] P. Sagaut, S. Deck, and M. Terracol, (2013). Multiscale and Multiresolution Approaches in Turbulence, 2nd edition (Imperial College Press, London, UK).

[10] C. G. Speziale, (1996). Computing non-equilibrium turbulent flows with time-dependent RANS and VLES, in *Proceedings of the 15th International Conference on Numerical Methods in Fluid Dynamics*, pp. 123–129.

[11] P. Spalart, W.-H. Jou, M. K. Strelets, and S. Allmaras, (1997). Comments on the feasibility of LES for wings, and on a hybrid RANS/LES approach, in *Proceedings of the First AFOSR International Conference on DNS/LES, Advances in DNS/LES*, pp. 137–147.

[12] S. S. Girimaji, R. Srinivasan, and E. Jeong, (2003).PANS Turbulence model for seamless transition between RANS and LES: fixed-point analysis and preliminary results,*in Proceedings of the 4th ASME-JSME Joint Fluids Engineering Conference*, pp. 1–9.

[13] F. R. Menter, M. Kuntz, and R. Bender, (2003). A scale-adaptive simulation model for turbulent flow predictions,

in 41st Aerospace Sciences Meeting and Exhibit, pp. 1–11.
[14] F. R. Menter and Y. Egorov, (2010). The scale-adaptive simulation method for unsteady turbulent flow predictions. part 1: Theory and model description, *Flow, Turbul. Combust.*, vol. 85, no. 1, pp. 113–138, Jun. 2010.
[15] M. L. Shur, P. R. Spalart, M. K. Strelets, and A. K. Travin. (2008). A Hybrid RANS-LES Approach With Delayed-DES and Wall-Modelled LES Capabilities. *International Journal of Heat and Fluid Flow*. 29:6. 1638-1649.
[16] B. J. Perot and J. Gadebusch, (2007). A self-adapting turbulence model for flow simulation at any mesh resolution, *Phys. Fluids*, vol. 19, no. 11, pp. 1–11.
[17] M. S. Gritskevich, A. V. Garbaruk, J. Schutze, F. R. Menter, (2012). Development of DDES and IDDES Formulations for the k-ω Shear Stress Transport Model. *Flow, Turbulence and Combustion*. 88(3). 431–449.
[18] S. B. Pope, (1975). A more general effective-viscosity hypothesis, *Journal of Fluid Mechanics*, vol. 72, no. 2. pp. 331–340.
[19] G. Lenci and E. Baglietto, (2015). A Structure-Based Approach for Topological Resolution of Coherent Turbulence: Overview and Demonstration, in *16th Int. Top. Meet. Nucl. React. Therm. Hydraul.*, Chicago, IL, USA, pp. 1–14.
[20] Baglietto and H. Ninokata, (2006). Anisotropic Eddy Viscosity Modeling for Application to Industrial Engineering Internal Flows, *Int. J. Transp. Phenom.*, vol. 8, no. 2, pp. 85–101.
[21] E. Baglietto and H. Ninokata, (2007). Improved turbulence modeling for performance evaluation of novel fuel designs, *Nucl. Technol.*, vol. 158, no. 2, pp. 237–248.
[22] T. Shih, J. Zhu, and J. L. Lumley, (1993). A Realizable Reynolds Stress Algebraic Equation Model, *NASA Technical Memorandum 105993*, pp. 1–34,.
[23] D. A. Lyn, S. Einav, W. Rodi, and J.-H. Park, (1995). A laser-Doppler velocimetry study of ensemble-averaged characteristics of the turbulent near wake of a square cylinder, *J. Fluid Mech.*, vol. 304, pp. 285–319.
[24] F. Lien, W. Chen, and M. Leschziner, (1996). Low-Reynolds-number eddy-viscosity modelling based on non-linear stress-strain/vorticity relations, *in Proceedings of the 3rd symposium on Engineering turbulence modelling and Experiments*, vol. 3, pp. 91–100.
[25] G. Lenci (2016). *A methodology based on local resolution of turbulent structures for effective modeling of unsteady flows*. Massachusetts Institute of Technology PhD Thesis.
[26] Meneveau, C., Lund, T.S., Cabot, W.H., (1996). A Lagrangian dynamic subgrid-scale model of turbulence. *J. Fluid Mech*. *319*, 353-385.
[27] Greg Ahmed, Ramm, Faltin, (1984). Some Salient Features of The Time-Averaged Ground Vehicle Wake, *in: Some Salient Features Of The Time-Averaged Ground Vehicle Wake*. doi:10.4271/840300
[28] Ashton, N., Revell, A., (2015). Key factors in the use of DDES for the flow around a simplified car, *International Journal of Heat and Fluid Flow* 54, 236–249.
[29] Ashton, N., West, A., Lardeau, S., Revell, A., (2015). Assessment of RANS and DES methods for realistic automotive models, *Computers and Fluids* 128, 1-15
[30] F. Menter and M. Kuntz (2004). Adaptation of eddy-viscosity turbulence models to un- steady separated flow behind vehicles, in *The Aerodynamics of Heavy Vehicles: Trucks, Buses, and Trains*, pp. 339–352.